

# Comparison of Chemically and Electrochemically Prepared Polyaniline Films. 2. Optical Properties

Douglas Chinn and Joel DuBow

Department of Materials Science and Engineering, University of Utah,  
Salt Lake City, Utah 84112

Jing Li, Jiří Janata, and Mira Josowicz\*

Material and Chemical Sciences Center, Pacific Northwest Laboratory,<sup>†</sup>  
Richland, Washington 99352

Received January 24, 1995. Revised Manuscript Received April 26, 1995<sup>⊗</sup>

Relaxation phenomena in thin polyaniline films synthesized chemically and electrochemically are investigated by UV–vis and IR spectroscopy. It is shown that the relaxation process carried out from the electrochemically oxidized or electrochemically reduced states of the polyaniline always proceeds toward the emeraldine state. The relaxation process in acid is governed by disproportionation and formation of semiquinone radicals. The changes in the population density of the polaronic states within the polaronic band allows determination of the change in the oxidation state and consequently the change in the position of the Fermi energy level. The formation of polaronic states is ascertained by diffusion of ions from or into the polyaniline matrix in solution and within the polymer in air.

## Introduction

Motivation for this work came from the realized need to prepare thin films of polyaniline on insulating substrates. Under those circumstances it is not possible to use the obvious electrochemical preparation route. The key question that needs to be answered is then the comparison of properties the chemically and electrochemically prepared polyaniline. In part 1,<sup>1</sup> we reported on the observed changes in work function and resistance with time. They are thought to be controlled by relaxation which drives the changes to an equilibrium state while maintaining the electroneutrality condition.<sup>2</sup> In part 2 we describe the relaxation behavior as followed by the optical properties of this material. A body of work exists on UV–vis spectra,<sup>3–13</sup> IR spectra,<sup>14–21</sup>

theoretical band calculations, and band diagrams derived empirically from UV–vis data.<sup>3,5,7,8,22–24</sup> Small differences between reported and our spectroscopic data are mainly due to different synthetic conditions and different processing treatments.

The polyaniline general formula is  $[-(B-NH-B-NH)_y(B-N=Q=N-)]_{1-y}n-$ , where B denotes a benzoid reduced unit and Q a quinoid oxidized unit. Definitions are given in Figure 1a. The basic undoped or acidic doped forms are labeled as amine (A) and salt (S) forms, respectively.<sup>25,26</sup> The repeat units of this copolymer can be assigned to the dimeric benzoid structure containing two benzoid rings (1A) and to the benzoid–quinoid segment containing one benzoid and one quinoid ring (2A) or, when doped with a protonic acid, 1S and 2S (Figure 1b). Both types of segment contribute to the redox state of the polymer.<sup>12,27</sup> In a perfectly ordered relaxed form the doped polymer chain would be in the emeraldine state which consists of alternating 1A and

\* To whom correspondence should be addressed.

<sup>†</sup> Pacific Northwest Laboratory is a multiprogram national laboratory operated by Battelle Memorial Institute for the U.S. Department of Energy under Contract DE-AC06-76RLO #1830.

<sup>⊗</sup> Abstract published in *Advance ACS Abstracts*, July 1, 1995.

(1) Chinn, D.; DuBow, J.; Liess, M.; Josowicz, M.; Janata, J. *Chem. Mater.*, previous paper in this issue.

(2) Daikhin, L. I.; Levi, M. D. *J. Chem. Soc., Faraday Trans.* **1992**, *88*, 1023.

(3) Huang, W. S.; MacDiarmid, A. G. *Polymer* **1993**, *34*, 1833.

(4) Yue, J.; Wang, Z. H.; Cromack, K. R.; Epstein, A. J.; MacDiarmid, A. G. *J. Am. Chem. Soc.* **1991**, *113*, 2665.

(5) Stafstrom, S.; Sjogren, B.; Bredas, J. L. *Synth. Met.* **1989**, *29*, E219.

(6) Cao, Y. *Synth. Met.* **1990**, *35*, 319.

(7) Stafstrom, S.; Bredas, J. L. *Mol. Cryst. Liq. Cryst.* **1988**, *160*, 405.

(8) Ohsawa, T.; Kabata, T.; Kimura, O.; Yoshino, K. *Synth. Met.* **1989**, *29*, E203.

(9) Cushman, R. J.; McManus, P. M.; Yang, S. C. *Makromol. Chem., Rapid Commun.* **1987**, *8*, 69.

(10) Cao, Y.; Smith, P.; Heeger, A. J. *Synth. Met.* **1989**, *32*, 263.

(11) Sun, Y.; MacDiarmid, A. G.; Epstein, A. J. *J. Chem. Soc., Chem. Commun.* **1990**, 529.

(12) Heeger, A. J.; Smith, P. In *Conjugated Polymers*; Bredas, J. L., Silbey, R., Eds.; Kluwer Academic Publishers: Dordrecht, 1991; p 141.

(13) McCall, R. P.; Ginder, J. M.; Leng, J. M.; Ye, H. J.; Manohar, S. K.; Masters, J. G.; Asturias, G. E.; MacDiarmid, A. G.; Epstein, A. J. *Phys. Rev. B* **1990**, *41*, 5202.

(14) Harada, I.; Furukawa, Y.; Ueda, F. *Synth. Met.* **1989**, *29*, E303.

(15) Ohsaka, T.; Ohnuki, Y.; Oyama, N.; Katagiri, G.; Kamisako, K. *J. Electroanal. Chem.* **1984**, *161*, 399.

(16) Tang, J.; Jing, X.; Wang, B.; Wang, F. *Synth. Met.* **1988**, *24*, 231.

(17) Kim, Y. H.; Foster, C.; Chiang, J.; Heeger, A. J. *Synth. Met.* **1989**, *29*, E285.

(18) Asturias, G. E.; MacDiarmid, A. G.; McCall, R. P.; Epstein, A. J. *Synth. Met.* **1989**, *29*, E157.

(19) Sariciftci, N. S.; Bartonek, M.; Kuzmany, H.; Neugebauer, H.; Neckel, A. *Synth. Met.* **1989**, *29*, E193.

(20) Monkman, A. P.; Adams, P. *Synth. Met.* **1991**, *41–43*, 891.

(21) Furukawa, Y.; Ueda, F.; Hyodo, Y.; Harada, I.; Nakajima, T.; Kawagoe, T. *Macromolecules* **1988**, *21*, 1297.

(22) Stafstrom, S.; Bredas, J. L.; Epstein, A. J.; Woo, H. S.; Tanner, D. B.; Huang, W. S.; MacDiarmid, A. G. *Phys. Rev. Lett.* **1987**, *59*, 1464.

(23) Genies, E. M.; Lapkowski, M. *J. Electroanal. Chem.* **1987**, *220*, 67.

(24) Euler, W. B. *Solid State Commun.* **1986**, *57*, 2447.

(25) Chiang, J.-C.; MacDiarmid, A. G. *Synth. Met.* **1986**, *13*, 193.

(26) Huang, W.-S.; Humphrey, B. D.; MacDiarmid, A. G. *J. Chem. Soc., Faraday Trans. 1* **1986**, *82*, 2385.

(27) Aoki, K. *J. Electroanal. Chem.* **1992**, *334*, 279.

(28) MacDiarmid, A. G.; Chiang, J. C.; Richter, A. F.; Epstein, A. J. *Synth. Met.* **1987**, *18*, 285.

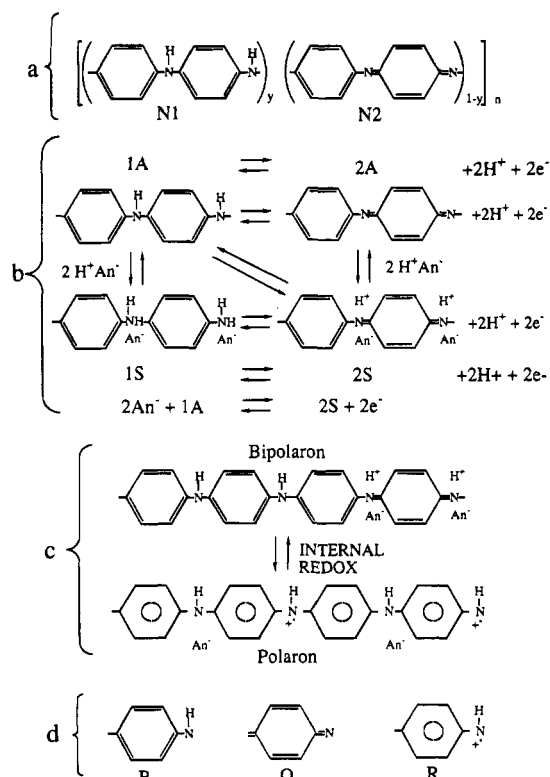


**Figure 1.** Different forms of polyaniline. (a) Generalized structure.  $y$  represents the oxidation state. N1 and N2 represent the benzenoid and quinoid dimeric subunit segments. (b) Redox reactions in polyaniline. All reactions can be taking place simultaneously.  $An^-$  represents the counterion which must be present to maintain charge balance. (c) Localized bipolaron to delocalized polaron redox reaction. (d) Three optically active forms of the ring structure. B is the benzenoid form, Q is the quinoid form, and R is the radical cation form of the benzene ring of the polymer backbone.

2S segments. This is the form of polyaniline with the highest conductivity.

The nitrogen atoms can be protonated, depending on the redox state of the polymer and the pH of the doping solution. The imine  $=N-$  nitrogens are preferentially protonated over the amine  $-NH-$  nitrogens, even though the amine form is more basic, probably due to steric hindrance of the adjacent phenyl ring.<sup>25</sup> The 1S structure probably only exists for very low pH doping, or it may exist during the initial stages of electrochemical oxidation of leucoemeraldine.<sup>26</sup> The 1S state is not stable in air and spontaneously oxidizes to a state near emeraldine.<sup>3</sup> Furthermore, both the 1S and 2S can exist as singly (1S', 2S') or doubly protonated (1S'', 2S'').<sup>25,26</sup> Elemental analysis comparing the anion/nitrogen ratio usually indicates that the polymer is not doped enough to form 1S units,<sup>29</sup> even for  $pH = -4$ . The 1S form is too acidic to be stable.<sup>23</sup>

**Doping of Polyaniline.** For a polymer chain of a total of  $N$  number density of polymer segments, it can consist of  $N1$  segments that are either 1A or 1S, and  $N2$  segments that are either 2A or 2S, thus  $N = N1 + N2$ . In the perfectly ordered emeraldine state  $N1 = N2 = N/2$ . Consequently the occupancy parameter has been defined as  $X = N1/N2$  (Figure 1a). For the intermediate

**Table 1<sup>a</sup>**

peak energy, eV	origin	ref
1	polaron intraband ES, R	3
1.5	valence-polaron band ES	
	$\pi_B - \pi_R$ (R)	3
1.8	quinone-diimine PB	3
2.0-2.2	$\pi_B - \pi_Q$ EB	3, 4, 5
	exciton	30
	PS bipolaron	6
2.2-2.3	$\pi_B - \pi_Q$ PB	6, 11
2.7-2.9	low valence levels to polaron band ES	3
	bipolaron	7
3.4	positive bipolaron	5
3.5	bandgap PB	6
3.5	$\pi - \pi^*$ bandgap ES	8, 29
3.6-4	$\pi - \pi^*$ bandgap EB, LB	3, 9, 13
4.1-4.2	$\pi - \pi^*$ bandgap LS	3
4.1-4.3	bandgap PS	6

<sup>a</sup> EB = emeraldine base (1A2A). ES = emeraldine salt (1A2S). PB = pernigraniline base (2A2A). PS = pernigraniline salt (2A2S) or (2S2S). LB = leucoemeraldine base (1A1A). LS = leucoemeraldine salt (1A1S) or (1S1S). bipolaron = (1A2S). polaron = (R)

state, when  $X = 1$ , the polymer is in the half-oxidized polymer form, where  $y = 0.5$ , resulting in the highest conductivity. For the completely reduced leucoemeraldine state,  $X \rightarrow \infty$  ( $y \rightarrow 1$ ) and for completely oxidized pernigraniline state,  $X \rightarrow 0$  ( $y \rightarrow 0$ ). The polymer becomes more insulating the farther it is driven from  $X = 1$ . Assuming that the total number of segments  $N$  is not changing during the relaxation process of the polymer, the distribution of 1A, 1S, 2A, and 2S segments before and after relaxation should represent the change in the redox state of the polymer as it relaxes or is doped.

Since the electron-donating effect of the 2S structure plays an important role in the conduction of PANi, it is important to examine the various equilibria (Figure 1b, c) upon electrochemical reduction or oxidation of emeraldine salt or upon protonation of emeraldine base. The 1A-2S dication or bipolaron is known to be unstable and undergoes an internal redox reaction to the radical cation, or polaron state<sup>29</sup> (Figure 1c). The different ring structures are electronically active and therefore can be identified in the UV-vis and IR spectra, which support a material with two regions, one insulating and one conducting. The optically active structures are defined in Figure 1d, where B = benzenoid ring, Q = quinoid ring, and R = radical cation. To maintain charge balance, anions,  $An^-$ , must accompany the movement of proton into or out of the polymer.

The various states of polyaniline absorb in the UV-vis region at several different energies (Table 1). When the polymer is fully reduced in the undoped 1A-1A leucoemeraldine base (LB) form, it absorbs photons at approximately 3.9 eV.<sup>9,13</sup> That absorption band represents the  $\pi - \pi^*$  antibonding transition and therefore is commonly associated with the width of the energy bandgap. This is a useful concept even though we discuss localized charge states using collective excitation terminology. In the partially oxidized undoped emeraldine base (EB) 1A-2A state, the bandgap is similar and a new absorption band appears around 2 eV, attributed to an exciton state. The excitonic transition results from an intrachain absorption leading to the formation of a "molecular" exciton which is a positive charge on adjacent benzenoid units and is bound to the

(29) Epstein, A. J.; Ginder, J. M.; Zou, F.; Bigelow, R. W.; Woo, H.-S.; Tanner, D. B.; Richter, A. F.; Huang, W.-S.; MacDiarmid, A. G. *Synth. Met.* **1987**, *18*, 303.

negative charge centered on the quinoid ring.<sup>4</sup> The exciton<sup>30</sup> has been associated with a distortion of the backbone of the polymer. The fully oxidized pernigraniline base (PB) 2A–2A state of the undoped polymer shows an intense band around 2.3 eV which is attributed to the  $\pi_B \rightarrow \pi_Q$  transition and a bandgap of 3.5 eV.<sup>11</sup>

Upon protonation of leucoemeraldine base to leucoemeraldine salt (LS) (1S–1S) the bandgap increases to  $\sim 4.1$  eV.<sup>3</sup> No lower energy absorptions were reported. Pernigraniline salt (PS) (2S–2S) shows an intense absorbance around 2 eV and a bandgap near 4.1 eV.<sup>6</sup>

Protonation of 1A2A emeraldine base to 1A2S emeraldine salt using an acid with  $\text{pH} < 1$  has been intensively studied in both air and solution. Results, as with all polyaniline data, vary somewhat due to the conditions of preparation of the polymer. At high protonation levels in emeraldine, the 2 eV band completely disappears into a 1.5 eV band, consistent with the disappearance of quinoid units to form the semiquinoid structures along the polymer chain. The 1.5 eV absorption band is then assigned to the  $\pi_B \rightarrow \pi_R$  transition where R is the radical cation excitation to the polaronic band formed in the bandgap.<sup>3,31</sup> (Note that S is not used in this work as is common in the literature to avoid confusion with 1S and 2S.) The valence band at 2 eV has an electron removed from the benzenoid ring, moves higher within the gap, and forms the polaron band. The resulting half-occupied polaron band has been calculated to be 1.0 eV<sup>22</sup> in width. This phenomenon is consistent also with the distortion of the orbital structure due to a chain conformation related process which leads to a new optical transition around 2.8–2.9 eV. That transition results from another low-lying  $\pi_B \rightarrow \pi_R$  excitation to the polaronic band which increases in magnitude with increasing number of semiquinoid structures.

Emeraldine salt is known to have a finite density of states at the Fermi level ( $E_f$ ),<sup>29</sup> consistent with  $E_f$  being within the polaron band in conducting emeraldine salt. There are low energy absorbances below 1.5 eV, usually attributed to an intrachain or intraband absorption within the polaron band. An absorbance at 1.78 eV is attributed to a nonhomogeneous distribution of deprotonated quinone–imine (2A) segments within the polymer chain.<sup>3</sup> Some authors<sup>8,23</sup> use polaron or bipolaron anti bonding levels to account for some absorbances.

Structural analysis of polyaniline films by chromatic behavior allows the determination of the previously defined occupancy parameter,  $X$ . It is a relative change of a characteristic absorption intensity,  $\Delta A/A$ , within a time period defined from  $t$  to  $t'$ :

$$X = \Delta A/A = (A_{t'} - A_t)/A_t \quad (1)$$

where  $A$  is the maximum in the 1.5–1.8 eV absorption band related to the transition of the quinoid to benzenoid segments during reduction or benzenoid to quinoid segments during oxidation. In the figures below the relaxation or doping time  $t'$  is counted from the beginning of the experiment, and the total time for the experiment is  $t$ .

Polyaniline has infrared absorbances around 1500  $\text{cm}^{-1}$  which is characteristic of the benzenoid ring, and another absorbance around 1600  $\text{cm}^{-1}$  which is characteristic of the quinoid state.<sup>14</sup> An absorbance at 1620  $\text{cm}^{-1}$  is indicative of the C=N bond,<sup>15</sup> and the semiquinone radical absorbs at  $\sim 1560$  and 1472  $\text{cm}^{-1}$ .<sup>14</sup>

The determination of the relative changes of the benzenoid and quinoid segments in PANiC or PANiE films as a function of time in solution and air forms the basis of this paper.

## Experimental Section

PANiC films and the PANiC/PANiE sandwich films were fabricated as described in part 1.<sup>1</sup> All potentials refer to a saturated calomel electrode (SCE). A platinum wire was used as an auxiliary electrode when the films were examined in solution. The voltammetric experiments were conducted with a EG&G Model 273 potentiostat/galvanostat (PAR).

Undoped PANiC films were immersed in 1 M  $\text{H}_2\text{SO}_4$  to observe changes during doping. To observe changes during solution relaxation, a previously doped film was first cycled at 30 mV/s in 1 M  $\text{H}_2\text{SO}_4$  five times between  $-100$  and 750 mV and stopped at 750 mV or at  $-100$  mV for 1 min. After that the electrochemical cell was disconnected and the open cell potential,  $E_{oc}$ , and the UV–vis spectrum was recorded simultaneously. The relaxation period was counted from the time the electrochemical cell was disconnected.

The relaxation in air was carried out after the films were oxidized or reduced as described in part 1, stopping the potential at either +750 or at  $-100$  mV. The films were removed from the acid after 10 s, rinsed and dried. They were put immediately into the spectrophotometer, and the spectrum was recorded. All spectra are relative to an uncoated quartz substrate. After 20 h in air, the spectrum was recorded again.

The UV–vis spectra in air were recorded on a Perkin-Elmer Lambda 6 spectrophotometer using films spun on quartz which had a pattern of platinum on it. The platinum allowed the polymer to be connected electrically to a potential source but had a 0.15 cm wide channel in the middle so that transmission spectrum could be observed without interferences from any metallic intermediate layer. The quartz transmits from 4.0 to 1.4 eV. We believe that this is the first time that spectroelectrochemical investigation of polyaniline was done on an insulating, nonmetallic substrate.

Borosilicate glass substrates were used with a Cary 5 (Varian) spectrophotometer when the UV–vis measurements were done in solution. The cell comprised a 1 cm cuvette (Aldrich) holding the spin-coated PANiC on a substrate as described above. The data were collected with an IBM/AT286 computer. The borosilicate glass transmits from 3.5 to 1.5 eV.

For IR spectroscopy a Nicolet Magna IR 550 spectrometer was used. Chips were the same as described in part 1, except that no nitride film was used. The oxide was etched off in hydrofluoric acid. The metal pattern acted as a mask, so the metal was still isolated from the substrate, but silicon channels existed between the metal leads. PANiC films were spun onto substrates as described previously, and PANiE films were grown on top of the spun films, allowing spectroscopic studies of the electrochemical material without using a metallic substrate. The IR beam was incident on the space between the leads. Films were polarized in solution, rinsed and dried, and put in the spectrometer under  $\text{N}_2$  for 15 min before the spectrum was taken, therefore, some of the initial relaxation information was lost. Silicon background spectrum was subtracted automatically from the silicon/polymer spectrum.

## Results

**Undoped to Doped Transition.** The UV–vis spectrum for an undoped PANiC film during immersion doping in 1.0 M  $\text{H}_2\text{SO}_4$  solution is shown in Figure 2. The solid line represents the spectrum of a PANiC film

(30) Duke, C. B.; Conwell, E. M.; Paton, A. *Chem. Phys. Lett.* **1986**, *131*, 82.

(31) Epstein, A. J.; MacDiarmid, A. G. *Mol. Cryst. Liq. Cryst.* **1988**, *160*, 165.

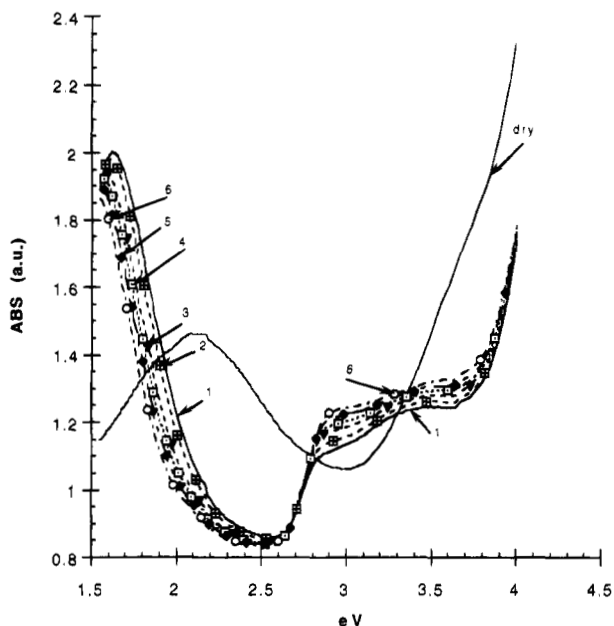


**Figure 2.** Changes in optical absorption spectrum of a PANiC film during solution doping. The spectra were recorded at various time intervals within the total immersion time of 120 min in 1 M H<sub>2</sub>SO<sub>4</sub>. Curve 1 is time  $t' = 0$ , curve 2  $t' = 10$  min, curve 3  $t' = 20$  min, curve 4  $t' = 30$  min, curve 5  $t' = 60$  min, and curve 6  $t = 120$  min. The spectrum of a dry PANiC film before immersion in the solution is also shown for comparison.

recorded in air before the film was immersed in sulfuric acid. It corresponds to those already reported in the literature.<sup>32</sup> The spectrum of undoped PANiC has one absorption band around 2.1 eV and a long absorption tail starting above 4.0 eV. These correspond to the 2A and 1A segments of the deprotonated emeraldine base.

Upon immersion in 1.0 M H<sub>2</sub>SO<sub>4</sub> the protonation of the imine groups causes the appearance of two new absorption bands around 1.7 and 2.9 eV (curve 1). These two new absorbances can be attributed to transitions from the valence band to the new polaron band which forms in the gap.<sup>22,31</sup> The lower energy band is due to charge separation between chains.<sup>10</sup> An additional band which cannot be seen by our experimental setup at 1.0 eV is due to an intrachain excitation.<sup>10</sup>

The decrease of the population of the 2S segments with time at 1.7 eV and the shift to lower energy is caused by the tendency of the 1A and 2S units to form semiquinone radical cations along the polymer chain. Within the energy range from 2.8 to 3.5 eV the absorption intensity is increasing with the immersion time,  $t'$ . The 2.8 eV absorbance is due to transitions from low-lying valence levels into the new polaron band.<sup>3</sup> Therefore, the increase in the absorption intensity corresponds to a density increase of semiquinone structures in the PANiC film. Consequently, their concentration determines the degree of oxidation of the polymer,  $X$ . The decrease in energy of the 1.7 eV peak to 1.5 eV and below indicates localized bipolarons becoming delocalized and forming polarons. Note that  $X$ , as measured by relative peak heights in optical data does not necessarily represent  $y$ , the actual oxidation state of the polymer, because to determine  $y$  optically the areas under the appropriate peaks need to be determined. Changes in  $X$  are therefore relative.

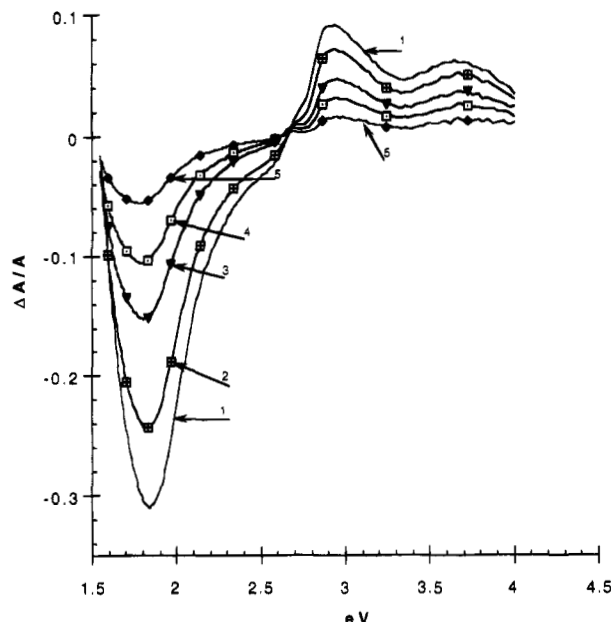


**Figure 3.** Relative absorption change,  $\Delta A/A$ , obtained from Figure 2 by applying eq 1 as defined in the text. Times are relative to  $t = 120$  min. The times for curves 1–5 are defined in the caption of Figure 2.

Protonic doping involves insertion of anions to preserve the electroneutrality in the polymer. The transition around 3.5 eV represents the bandgap of the polaronic state, excitations to the 1A or 1S level.<sup>29</sup> The ratio of the intensity of the absorbance maxima at 1.7 and 3.5 eV reflects the change in the oxidation state. Thus  $X$  is increasing with immersion time from approximately  $X = 0.60$  to 0.70 and suggests that charge redistribution occurs in PANiC upon immersion in sulfuric acid. The increased value of  $X$  indicates that doping reduces the film. Furthermore, the decreasing value of the measured open-cell potential  $E_{oc}$  during the doping process accounts for interfacial processes within the polymer and at the polymer/solution interface. Resistance values were not measured during solution doping because any potential or current applied to measure resistance would change the oxidation state of the polymer.<sup>33</sup>

The change in the oxidation state of the polymer is governed by the disproportionation reaction,  $\Delta(1A) + \Delta(2S) \rightarrow 2\Delta R^*$ , where  $\Delta R^*$  is the semiquinone radical cation, or polaron. It is possible to evaluate the change in the concentration of 1A and 2S segments by applying eq 1. Figure 3 represents the change in the relative absorption,  $\Delta A/A$ , during immersion doping where the absorption change,  $\Delta A$ , is normalized for the absorption intensity of the fully doped state of the polymer, corresponding to a doping period of  $t = 120$  min. There are two isosbestic points at 2.7 and 1.6 eV which separate three different chromophoric systems. The isosbestic points confirm the existence of the equilibrium state. The decrease in absorbance around 1.7 eV is due to 2S segments becoming radical cations. Simultaneous increase of absorbance at 2.9 eV is also due to an increasing number of polarons in the film. Spectra of undoped and doped films in air show similar behavior.

**Relaxation in Sulfuric Acid after Polarization.** Electrochemically induced polarization of the doped

(32) Monkman, A. P.; Bloor, D.; Stevens, G. C.; Stevens, J. C. H. *J. Phys. D: Appl. Phys.* **1987**, *20*, 1337.

(33) Unpublished results

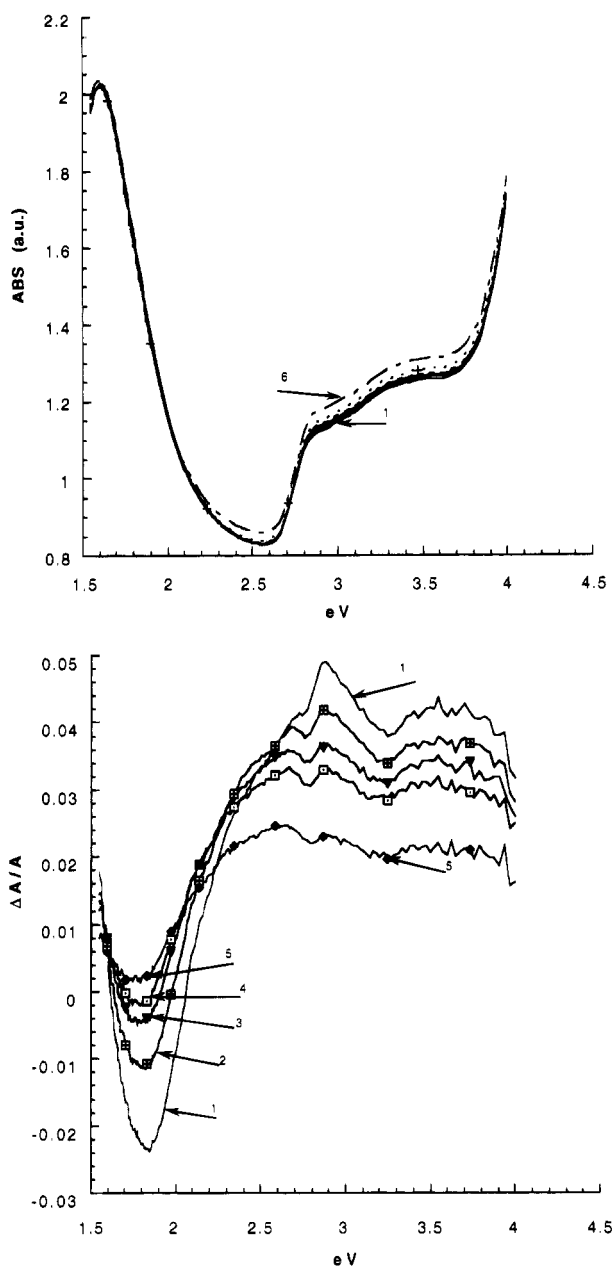


**Figure 4.** (a) Changes in optical absorption spectrum of a PANiC film in 1 M  $\text{H}_2\text{SO}_4$  after applying a polarization potential of +750 mV. The spectra are recorded at various time intervals during 120 min of relaxation. Times are as given in the caption of Figure 2. (b) Relative absorption change,  $\Delta A/A$  obtained from Figure 4a by applying eq 1 in the text. Times are the same as in Figure 3.

PANiC at +750 mV results in very small changes in the absorbance spectrum during relaxation for 120 min (Figure 4a). The ratio of the absorption intensities calculated for the 1.6 and 3.5 eV peaks is increasing with relaxation time from  $X = 0.54$  to 0.56. A slightly oxidized film spontaneously reduces toward the emeraldine state spectrum. The similarity of this spectrum with the emeraldine salt spectrum indicates that the film is not fully oxidized to pernigraniline or even to nigraniline at this oxidation potential. Quartz crystal microbalance (QCM) studies<sup>34</sup> indicate that the film loses mass near the end of the oxidation cycle, because the oxidation releases protons. The loss of protons

causes some anions to be expelled, but the oxidized film still has more mass than the emeraldine form does, at least immediately after oxidation. The film after oxidation is a random mixture of 1A, 2S, and R species, with an excess of acid present, possibly causing the formation of 1S species. The pH in the film can be higher than that in solution.<sup>35</sup>

Optical spectra normalized according to eq 1 (Figure 4), reveal the existence of 2.9 and 1.85 eV transitions, neither seen in Figure 4a. The 1.8–1.7 eV transition indicates the existence of the transition from the valence band to the bipolaron level in the bipolaronic band. The changes in the density ratio  $X$  between the 1A or 1S and 2S segments also results in splitting the 2.9 eV transition into an additional minor optical band around 2.7 eV. The shift in the position of the poorly defined isosbestic point near 2.1–2.3 eV may indicate changes resulting from charge equilibrium rearrangements taking place within the polaronic state. This observation agrees with the band structure calculations for protonated PANi which show very asymmetric valence and conduction bands and one half-occupied polaron band in the gap, instead of two bands as is usually found in other conducting polymers.<sup>22</sup> Thus relaxation in solution can be accounted for by an increase in the polaron concentration at the expense of 2S structure.

Electrochemical polarization of the protonated PANiC to  $-100$  mV results again in small changes in the absorbance spectrum in solution (Figure 5a). The ratio of the absorption intensity at 1.7 and at 3.5 eV is decreasing during relaxation time from  $X = 0.69$  to 0.62 indicating a spontaneous oxidation of the film. The normalized optical spectrum according to eq 1 (Figure 5b) reveals the existence of high population of undoped 2A segments which is reflected in the transition around 2 eV. The differential spectra are roughly opposite those from the oxidized state (Figure 4b). Quartz crystal microbalance measurements<sup>34</sup> indicate considerable loss of mass as the film is driven from the intermediate state to the reduced state consistent with a film low in dopant when the scan is stopped at  $-100$  mV. The rapid change from spectrum 1 (with a low point near 3 eV) to spectrum 2 is probably due to the uptake of dopant during the initial steps of relaxation. Again, these spectra reveal that the film is not fully reduced to the leucoemeraldine or even protoemeraldine. A weakly defined isosbestic point is seen near 2.8 eV. The development of the 1.6 eV peak from the 1.5 eV peak upon relaxation indicates partitioning of the states. The relative absorbance is above zero in all cases, and since  $N$  is constant, there must be a relative absorbance below zero below 1.5 eV, indicating an increase of polaronic states upon relaxation.

#### Comparison between Doping Levels Evaluated from the Open-Cell and Optical Measurements.

Figure 6 shows the correlation of the relative changes of the absorption  $\Delta A/A$  with the measured open cell potential,  $E_{oc}$ , for the 1.7 eV peak. Since  $E_{oc}$  is a property of the interface between the solution and the polymer, the correlation obtained reflects the development of an equilibrium state at the end of the relaxation process in sulfuric acid. The negative potential of  $-100$  mV applied causes an increase of  $E_{oc}$  until it reaches a

(34) Orata, D.; Buttry, D. A. *J. Am. Chem. Soc.* **1987**, *109*, 3574.

(35) Ghosh, S.; Vishalakshi, B.; Kalpagam, V. *Synth. Met.* **1992**, *46*, 349.

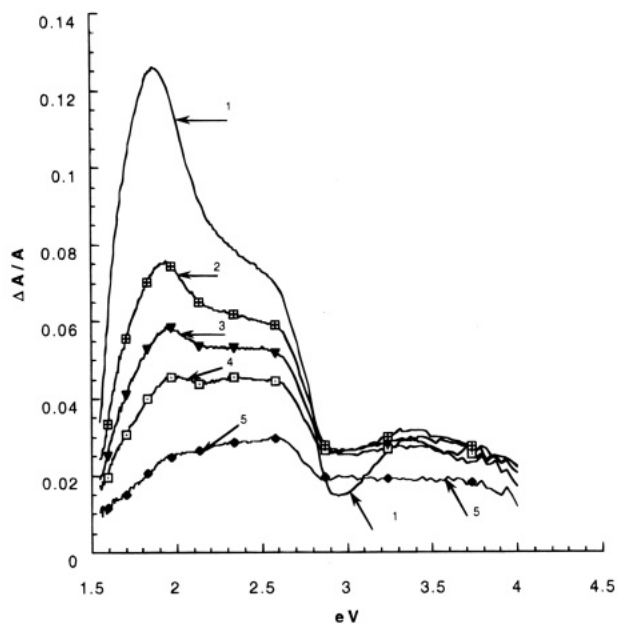
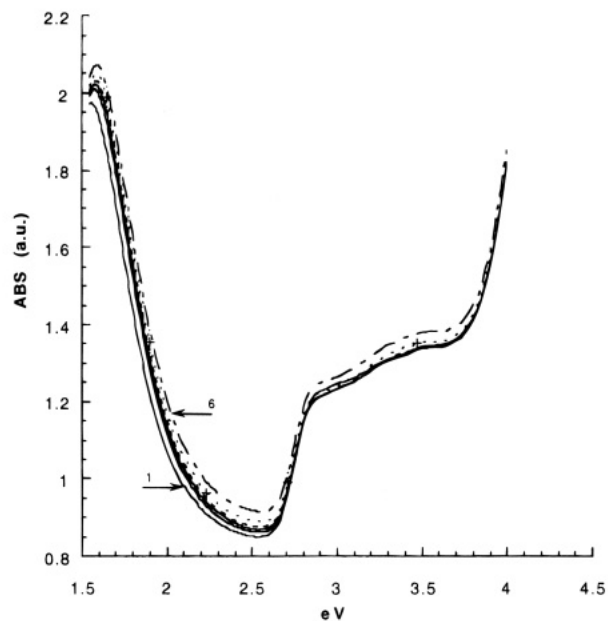


**Figure 5.** (a) Optical absorption spectrum of a PANiC film recorded at various time intervals within the total immersion time of 60 min in 1 M H<sub>2</sub>SO<sub>4</sub> after applying a polarization at -100 mV. Times are given in the caption of Figure 2. (b) Relative absorption change,  $\Delta A/A$  obtained from Figure 5a by applying eq 1 in the text. Times are the same as in Figure 3.

stable value of +490 mV. On the other hand, the applied positive potential of +750 mV causes  $E_{oc}$  to decrease with relaxation time until an equilibrium state at 500 mV is reached. The changes in the absorption intensities correlate with the  $E_{oc}$  changes. The  $\Delta A/A$  changes are much more pronounced from the reduced state of the PANiC film than from the oxidized state. The transitions of the film as it approaches equilibrium is related to the instability of 1A2S toward disproportionation and formation of two R structures.<sup>36</sup> In protonic doping, insertion of anions is also involved to preserve electroneutrality conditions.

**Transient Effects during Relaxation Carried out in Sulfuric Acid.** The linear dependence between the

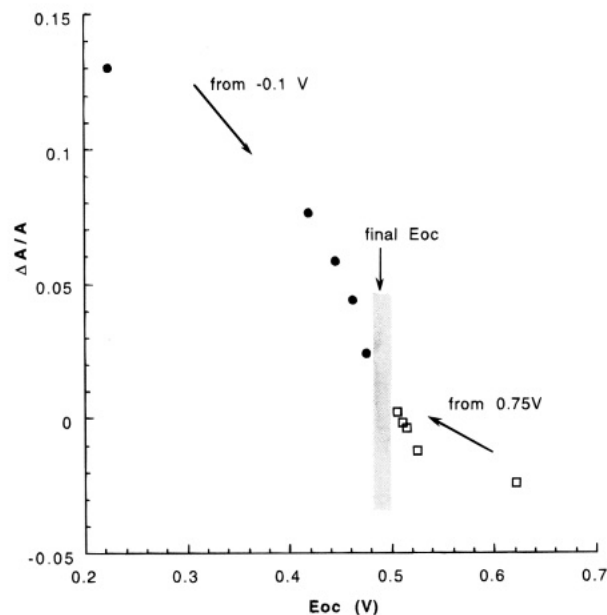


**Figure 6.** Correlation between  $\Delta A/A$  and the open cell potential,  $\Delta E_{oc}$ . The  $\Delta A/A$  values were obtained for the polarization from 750 mV for the transition at 1.8 eV (Figure 4b) and for the polarization from -100 mV for the transition at 1.9 eV (Figure 5b).

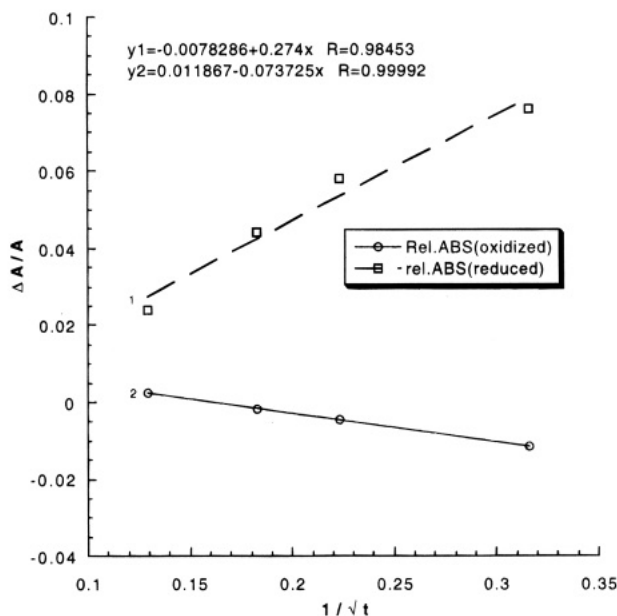


**Figure 7.** Changes in the relative absorbance,  $\Delta A/A$  during relaxation time  $t$  plotted vs  $t^{-1/2}$ . Curve 1 represents the changes from the oxidized state. Curve 2 represents the changes from the reduced state of the PANiC film. The  $\Delta A/A$  was obtained as the same way as in Figure 3.

changes in the relative absorbance,  $\Delta A/A$  of the 1.7 eV peak, and the inverse of  $t^{1/2}$  shown in Figure 7 indicates that the protonic doping or dedoping is diffusion controlled. The protonic doping occurs faster from the reduced state (curve 1) than does dedoping from the oxidized state (curve 2) of the PANiC film. The positive slope of 0.27, of curve 1, indicates a transfer of protons into the PANiC film. On the other hand, the protons are being depleted from the positively polarized PANiC with a slope of -0.07 (curve 2) allowing the formation of semiquinone radical cations. The difference in the slopes reflects the difference in kinetics of the two

(36) Leclerc, M.; Guay, J.; Dao, L. H. *Macromolecules* **1989**, *22*, 649.

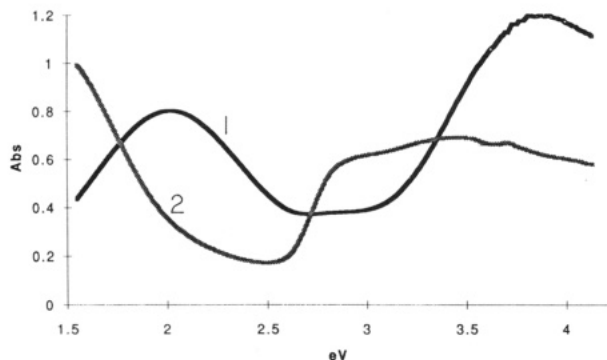


**Figure 8.** Comparison of optical spectra of PANiC film deposited on quartz substrate before (curve 1) and after immersion in 1 M  $\text{H}_2\text{SO}_4$  (curve 2) for 2 h. Both spectra were recorded in air.

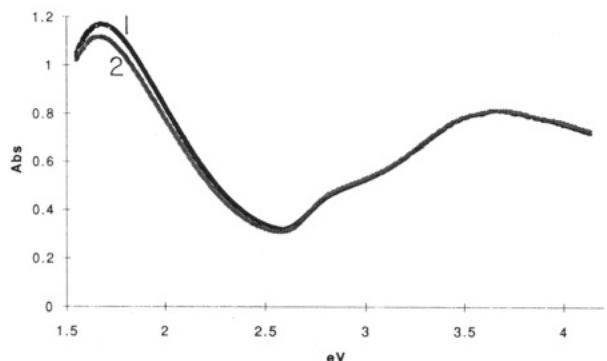


**Figure 9.** Absorbance of freshly oxidized PANiC film in air (curve 1) and the same film after 20 h (curve 2).

charge-transfer processes at the polymer/sulfuric acid interface.

#### Study of Doping Processes Carried out in Air.

Figure 8 shows the spectra of a PANiC film deposited on a quartz substrate in the emeraldine base form before and after immersion in 1 M  $\text{H}_2\text{SO}_4$  for 2 h. The optical spectra were recorded after short drying of the films in air as described in part 1.<sup>1</sup> The loss of the absorption intensity of the undoped PANiC film around 3.8 eV, in comparison with Figure 2, signals a change in the  $\pi$ - $\pi^*$  transition. The shift of the 2.1 eV transition of the undoped PANiC to lower than 1.5 eV in the doped PANiC suggests a development of a polaronic state. Furthermore, there are three isosbestic points at 1.75, 2.75, and 3.3 eV which reflect the existence of three different reaction equilibria that are driving the doping process.

**Relaxation Process in Air following an Electrochemical Polarization.** The changes in absorbance due to 20 h of relaxation in air of a PANiC film prepared in its oxidized (Figure 9) or reduced (Figure 10) state have been monitored. In air, water can enter or leave the film, but the acid cannot. A PANiC film as prepared in the oxidized state shows only a minor decrease in the population density of the 2S segments (at 1.7 eV) and minor shift to lower energies indicating an increased presence of the polaronic state. Almost no changes in the optical bandgap transition are seen around 3.7 eV. The oxidation degree,  $X$ , defined as the ratio of the absorption intensity at 3.7 and 1.7 eV transitions is changing from  $X = 0.66$  to 0.71, indicating spontaneous reduction. The rinsing and drying of these films eliminates excess acid and water. The work function decrease can be accounted for as the overoxidized polymer

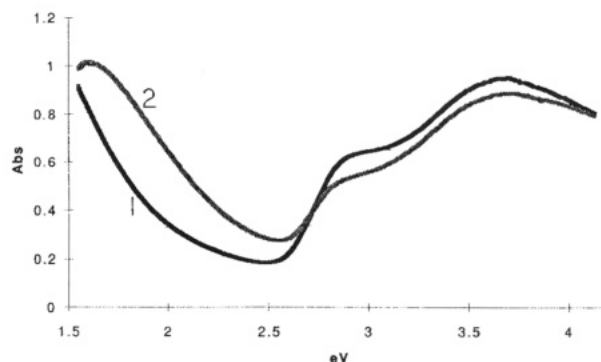


**Figure 10.** Absorbance of freshly reduced film in air (curve 1) and the same film after 20 h (curve 2).

develops more R character and the Fermi energy moves upward the forming polaron band.

On the other hand, the relaxation process of the PANiC film polarized electrochemically to  $-100$  mV results in much bigger changes in the optical spectra (Figure 10). This film is deficient in dopant acid. The absorption peak of the low energy transition is increasing in energy to a peak above 1.5 eV, indicating creation of quinone 2A or bipolaronic units, consistent with the increase of resistance seen during relaxation. The transitions at 3.6 and 2.8 eV are losing their optical absorption intensity indicating spontaneous oxidation of 1A units to 2A units, in accord with an increasing intensity near 2 eV. Ratio  $X$ , estimated from the absorption maxima at 3.6 and 1.7 eV, at the end of the relaxation process, is relatively high, approximately  $X = 0.85$ . The film is underdoped and slightly reduced, causing delocalized polarons to localize into bipolarons. Since the anion content cannot change in air relaxation, the carrier concentration must be constant. The bipolaron mobility will be lower than the polaron mobility, consistent with an increase in resistance during relaxation. The work function decrease is due to a rising Fermi energy as the bipolaron band forms out of the polaron band.

**Relaxation Process of a PANiC/PANiE Film in Air following an Electrochemical Polarization.** A PANiC/PANiE sandwich film behaves in air similarly to a PANiC film alone. Almost no changes in the absorbance were observed after 48 h relaxation in air for the PANiC/PANiE substrates polarized in sulfuric acid at  $+750$  mV. However, when the polymer sandwich was polarized at  $-100$  mV, the oxidation ratio due to relaxation in air reaches a high level of  $X = 0.8$  again as it was observed previously for the PANiC film alone.

**Changes in Infrared Absorbance during Relaxation and Differences between PANiC and PANiE.** The as-made and doped PANiC film shows relative peak heights of  $1482\text{ cm}^{-1}/1589\text{ cm}^{-1} = 0.76$ , representing the  $X$  ratio, which is high, similar to the UV-vis data. This ratio is merely the peak height ratio and does not determine the actual oxidation state. Figure 11 shows five spectra. The top spectrum, curve 1, is the as-made film. The  $1620\text{ cm}^{-1}$  peak is minor. The film transmits at  $1558\text{ cm}^{-1}$ . Additional benzenoid peaks are seen at  $1508$  and  $1493\text{ cm}^{-1}$ , and there are prominent peaks at  $1546$  and  $1552\text{ cm}^{-1}$  which is likely part of the benzenoid absorbance. Additional peaks are seen at  $1572$  and  $1472\text{ cm}^{-1}$  which belong to the semiquinone state. A shoulder to the quinoid absorbance at  $1565\text{ cm}^{-1}$  can be seen, but it is not distinct.

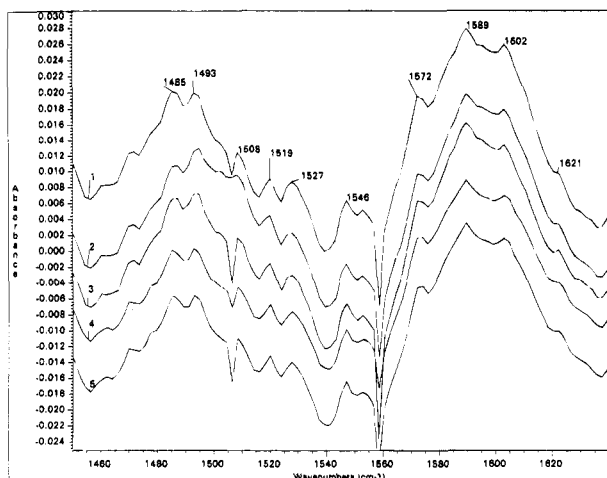


**Figure 11.** Infrared absorbance characteristics of polyaniline in air. Curve 1: Polyaniline film as made and doped with sulfuric acid. Curve 2: Film immediately after reduction. Curve 3: Reduced film after 20 h in air. Curve 4: Oxidized film immediately after oxidation. Curve 5: Oxidized film after 20 h in air.

Upon reduction, curve 2, the B peak shifts to higher wavenumber,  $1494\text{ cm}^{-1}$ , but the  $1589\text{ cm}^{-1}$  Q peak is constant. The  $X$  ratio of freshly reduced PANiC in air is 0.81, indicating that the film is more reduced than the original PANiC film. The  $1508\text{ cm}^{-1}$  peak gains in intensity and the absorbance from  $1494$  to  $1546\text{ cm}^{-1}$  generally broadens, indicating more benzenoid character. The C=N peak at  $1620\text{ cm}^{-1}$  also absorbs more after reduction, so the applied reduction potential causes major rearrangement of the microstructure of the polymer. The polymer has less R character than the as-made film.

After 48 h, curve 3, the B peak has shifted back to  $1482\text{ cm}^{-1}$ , and the occupancy parameter  $X$  (intensity ratio) has increased to 0.80, indicating the film is relaxing toward the emeraldine state. The biggest change upon relaxation is the prominence of the  $1620\text{ cm}^{-1}$  peak, indicating that the film is losing semiquinone character and developing quinoid character. This is consistent with the increase of resistance upon relaxation, and the concept of phase changes from an ordered semiquinone (polaron) structure to a less ordered quinoid (bipolaron) structure upon relaxation, where the bipolaron has lower mobility than the polaron. The relaxed spectrum resembles the as-made spectrum except for the prominence of the C=N peak.

Immediately after oxidative polarization, curve 4, the  $X$  ratio decreased to 0.75, indicating a general oxidation of the film. Also present is the same shift in the  $1482\text{ cm}^{-1}$  peak to  $1493\text{ cm}^{-1}$  and an increase in the  $1508\text{ cm}^{-1}$  peak as seen in the reduced material. The C=N peak at  $1620\text{ cm}^{-1}$  absorbs more, showing more quinoid character. The high resistance of this film is thus attributed to a high proportion of quinoid character after oxidation.

After 48 h, curve 5, the  $X$  ratio increases to 0.7, indicating a relaxation toward the emeraldine state, and the  $1482\text{ cm}^{-1}$  peak gains in intensity and the  $1493$  and  $1508\text{ cm}^{-1}$  peaks lose intensity, also indicating a return toward the emeraldine state. Changes, in the UV-vis spectrum, are small. There is an increase in the  $1472\text{ cm}^{-1}$  semiquinoid peak to account for the resistance decrease upon relaxation.

**Differences between PANiC and PANiE in the IR Spectrum.** To determine differences between PANiC and PANiE, a PANiC film's IR spectrum was recorded. PANiE was grown on the film in five-cycle increments, the IR spectra being recorded after each five cycles. The scan was stopped near 450 mV scanning anodically (the open-cell potential of the PANiC) to have the grown PANiE film in the emeraldine state to minimize relaxation related phenomena.

The  $X$  ratio decreases continuously with increasing thickness of PANiE, indicating a more oxidized character of the PANiE compared to the PANiC. The PANiE also shows more semiquinoid character than the PANiC film.

A second experiment was performed to compare the two types of PANi films. A 20-cycle PANiE film was grown, stopping the scan at 400 mV. The PANiE film and a PANiC film were put in 1 M  $\text{H}_2\text{SO}_4$  and held at 400 mV for 1 h to drive the two films to identical oxidation states. 400 mV was selected because of the higher conductivity of films at a potential somewhat below the standard  $E_{oc}$  of PANiC. The  $X$  ratio is very similar for the two films, but PANiE shows sharper peaks, indicating a more ordered structure. PANiC shows a stronger C=N absorbance, and thus the electrochemical material has more semiquinoid character than the chemical material.

**Estimation of Mobility.** The macroscopic conductivity of polyaniline is controlled by the continuous insulating phase. A total carrier density was calculated using a molecular weight of  $298\text{ g mol}^{-1}$  for a dimeric radical cation with a single sulfuric acid dopant molecule and a density of  $1.25\text{ g cm}^{-3}$ .<sup>37</sup> This assumes a 50% doping level.<sup>25,26</sup> The carrier concentration is  $N_c = 2.6 \times 10^{21}\text{ cm}^{-3}$  of dimers for this set of assumptions, which is the same as  $N$  above. This value is higher than those reported, which were based on device studies using toluene sulfonic acid as a dopant, of a carrier concentration of  $2.8 \times 10^{18}\text{ cm}^{-3}$ .<sup>38</sup> It is assumed that the volume of insulating material is half the total volume<sup>39</sup> (which is a high estimate for this particular polyaniline), so the actual carrier concentration is  $1.3 \times 10^{21}\text{ cm}^{-3}$ . A similar calculation<sup>40</sup> gave a carrier density of  $4 \times 10^{21}\text{ cm}^{-3}$ . On the basis of a conductivity of  $\sigma = Neu = 0.03\text{ S cm}^{-1}$ ,<sup>1</sup> the mobility  $u$  is calculated at  $1.4 \times 10^{-4}\text{ cm}^2\text{ V}^{-1}\text{ s}^{-1}$ . This rough calculation is in approximate agreement with mobility values published previously<sup>38</sup> of  $4.68 \times 10^{-4}\text{ cm}^2\text{ V}^{-1}\text{ s}^{-1}$ , where toluene-sulfonic acid was used as a dopant.

## Discussion

Major changes in optical spectra are seen after doping. The doping process results in the changes in population density of 1A, 1S, 2A, and 2S segments, all of which are related to the formation of semiquinone radical cations. The optical spectra before and after the doping allow identification of the polaronic and bipolaronic redox species. It was observed that during the doping

(37) Chartier, P.; Mattes, B.; Reiss, H. *J. Phys. Chem.* **1992**, *96*, 3556.

(38) Chen, S.-A.; Fang, Y. *Synth. Met.* **1993**, *60*, 215.

(39) Epstein, A. J.; Joo, J.; Kohlman, R. S.; Du, G.; MacDiarmid, A. G.; Oh, E. J.; Min, Y.; Tsukamoto, J.; Kaneko, H.; Pouget, J. P. *Synth. Met.* **1994**, *65*, 149.

(40) Pelster, R.; Nimitz, G.; Wessling, B. *Phys. Rev. B.* **1994**, *49*, 12718.



processes the relative oxidation level  $X$  was changing, depending on time.

Doping is defined as depopulating the  $\pi$  valence band of the polymer chain with no change in the number of electrons. This was accompanied by an increase of the density of polaronic states at energies below the 1.7 eV transition. The transition for the bandgap around 3.5 eV also loses absorption intensity suggesting a decrease in the  $\pi$ - $\pi^*$  interaction and providing a minor change in the position of the absorption maximum, due to the uppermost valence band becoming the polaron band, causing an apparent increase in the bandgap. The ratio  $X$  increases with time, indicating a slow reduction of the film in acid after the initial doping induced oxidation.

Since the bandgap energies of the polaronic state and of the bipolaronic state are very close in the different oxidation states, it is difficult to use the bandgap energy transition for the discussion of the Fermi energy level in the material.

Polyaniline relaxes in both air and in solution when driven from its equilibrium state by electrochemical polarization. The oxidation level was decreasing only while the PANiC film was relaxing after applying the reductive polarization. In the doping and oxidized relaxation processes the  $X$  value increases. An increase in the doping level is reflected in the electron donor behavior of the polymer. Changes in the density of 1A or 1S units to polaronic units contributes to the increased filling and widening of the polaronic band and a subsequent movement of the Fermi level. A shift of the polaronic transition from 1.8 eV to lower energy suggests a decrease in separation between the valence and polaron bands. By analogy a shift toward a higher transition energy can be related to an increase in separation between the two energy levels. Upon the relaxation process the system is accommodating or releasing electrons or holes which causes a lattice polarization. The lattice polarization is shifting the polaronic level to a higher energy level. Finally, a decrease of the transition energy from 2.85 to 2.7 eV

(Figure 3b) represents a separation decrease between the polaron level and the valence band. That change is related to the change of the Fermi energy level position. This is supported by the experimental results reported in part 1.<sup>1</sup>

The interaction of the PANiC with sulfuric acid after a negative polarization of the lattice results in the transition around 1.9 eV. The shift of that transition to higher transition energy (Figure 5) correlates with the protonic doping which forms the bipolaronic state. The insertion of holes into the valence band causes a decrease in the separation between the polaron level and the conduction band of the polaronic state. Consequently the Fermi energy level is rising and the work function is decreasing.

## Conclusions

In this paper we have pointed out that an extensive correlation between the distribution of the benzoid–quinoid and benzoid–benzoid segments exists. As a result of lattice relaxation the distribution of those segments is changing. This change reflects in the change of the oxidation level of polyaniline film. An increase of the oxidation level raises the position of the Fermi energy level. The redistribution process of the polarized 1A, 1S, and 2S segments depends only indirectly on the polarization state of the PANiC film. Much higher effect on the redistribution of the 1A and 2S states is observed during the doping process carried out in sulfuric acid. The PANiC/PANiE sandwich films behave in air in the same way as the PANiE film.

**Acknowledgment.** This work was supported in part by a grant from the Office of Exploratory Research of the Environmental Protection Agency. The authors would like to thank Dana Overacker of the Advanced Combustion Engineering Research Center for his assistance in collecting the infrared data.

CM950044K